Precise Phase-Based Ranging and Motion Detection for IoT By Reusing OFDM Data Subcarriers

Terry N. Guo, Wesam Al Amiri and Allen B. MacKenzie

Abstract—This paper investigates a precise ranging technique for IoT able to employ an extensive number of phases extracted from OFDM subcarriers including both pilot and data subcarriers. The authors focus on laying out an analytical framework backed up by experiment. The work is based on a bi-static or multi-static setup in the fashion of integrated sensing and communication (ISAC). The optimal range estimation rule and capability of micro motion monitoring are addressed. An optimal subcarrier selection method along with quantitative assessment of range ambiguity is provided. In particular, a decision-feedback phase extraction technique is introduced in order to make use of data subcarriers in addition to the pilot subcarriers. Phase noise characteristics measured on software defined radios (SDRs) are reported, confirming that the phase noise can be roughly viewed as an iid wide-sense stationary (WSS) Gaussian random process. Sensitivity of motion detection and estimation as well as range ambiguity assessment results measured in both norm of phase difference and pairwise error probability are provided.

Index Terms—Integrated Sensing and Communication (ISAC), Internet of Things (IoT), carrier-phase-based ranging and localization, motion detection, localization.

I. Introduction

Spurred partly by increasingly interest in Integrated Sensing and Communication (ISAC) [1], sensing functionalities have found many use cases. In the context of Internet of Things (IoT), sensing is especially useful–it can track targets (e.g., patients and elderly people) and monitor the environment (e.g., crowdedness and road traffic density), etc. Here "sensing" specifically refers to radio sensing, and under radio sensing umbrella there are a number of related topics, such as detection, ranging, localization, and target tracking, etc. From an ISAC perspective, the sensing functionalities can be made as "add-on bonus" on the existing communication infrastructure, without requiring another dedicated system. Motivated by many real world requests, research and applications in localization have received tremendous attention in the last two decades, and significant progress has been evidenced recently. With a number of coordinated receivers (anchors), a target's location can be estimated using different techniques. One family of source localization techniques are based on angle of arrival (AOA) or direction of arrival (DOA) [2], [3], and they require precise AOA measurement and line-ofsight (LOS) propagation. Alternatives to these angle-related techniques are a large family of range (or distance) based localization techniques which measure distances and then do data fusion to estimate the locations. The required ranges and range differences can be estimated using time of arrival (TOA) or time difference of arrival (TDOA) [4]–[6] as well as received signal strength (RSS) [7], [8]. However, many existing ranging and localization techniques consider targets with active signal sources. Also, some of these techniques are imprecise and challenging to achieve sub-wavelength accuracy. This is primarily because of limited power and bandwidth. Additionally, most research on motion sensing employs datadriven approaches, which involve training and inference based on a large volume of measurement data.

T. Guo is with the Center for Manufacturing Research, Tennessee Technological University, Cookeville, TN (email: nguo@tntech.edu).W. Al Amiri and A. MacKenzie are with the Dept. of Electrical and Computer Engineering, Tennessee Technological University, Cookeville, TN (email: {waalamiri42, amackenzie}@tntech.edu). This work is supported by the National Science Foundation under grant #2135275.

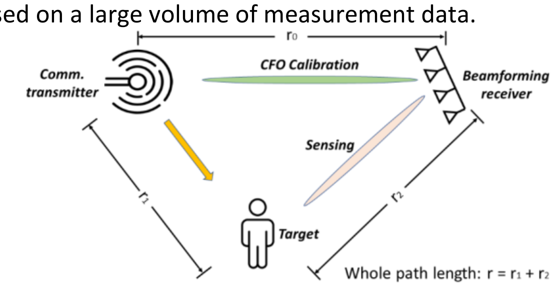

Fig. 1. Conceptual illustration of proposed system (showing only one receiver; CFO=Carrier Frequency Offset).

In this paper, we consider a bi-static or multi-static configuration with low-speed targets, and a precise ranging technique making use of multiple phases extracted from OFDM subcarriers (including both pilot and data subcarriers). As shown in Fig. 1, the configuration is similar to that of bistatic or multi-static radar, assuming the transmitter is able to steer its beam and direct-path interference can be avoided. Compared to active source ranging, it is very challenging to do sensing in such a bi-static or multi-static setup due to limited communication signal power and small radar cross section (RCS). On the other hand, when a target speed is relatively low, the Doppler frequency is close to zero, thus no information in the Doppler domain can be obtained practically due to insufficient Doppler resolution incurred by limited signal bandwidth (note that normal OFDM waveform is employed in this research). One interesting use case is proactive resource allocation/management using mobility information of passive targets. The target mobility may be tracked based on motion (small range displacement) instead of Doppler frequency.

Carrier-phase-based ranging [9]–[12] seems to be a proper approach for the scenario of our interest, if the phase noise can be suppressed effectively (discussion of existing work in this regard is omitted due to limited space in this paper). Phases at selected OFDM subcarriers are employed for ranging, and these subcarriers can be reserved for ranging only or for both communication and sensing. In the latter case, the reserved subcarriers deliver symbols that contain both data and range information, offering sensing functionality without significantly increasing system complexity and sacrificing communication performance. It can be seen in the following that phase noise is a performance-limiting factor for achieving precise ranging and micro motion monitoring. One promising strategy is to employ many subcarriers including data subcarriers. A decision-directed technique illustrated in Fig. 2 is designed to remove data symbols and extract range-based information from the data subcarriers. The major challenge for achieving a millimeter-level resolution is about how to effectively suppress the phase noise in phase estimation. Fortunately, with the decision-directed technique, as many "free" data subcarriers as possible can be used jointly to increase the signal-to-noise ratio (SNR), thanks to the orthogonality property of phase noise terms at different subcarrier frequencies.

Major contributions of this paper include: 1) an analytical framework for phase-based ranging is introduced and assessed using both analysis and experiment; 2) an optimal selection of subcarrier frequencies is formulated as a max-min optimization problem, and range ambiguity measured in pairwise error probability is evaluated against phase noise level; and 3) a decision-feedback phase extraction technique is proposed and experimentally examined. Calibration, beamforming, beam sweeping, localization and target tracking are beyond the scope of this paper, and we assume some prerequisite conditions have been met for the ranging process.

The rest of this paper is organized as follows. Problem formulation and analysis of phase-based ranging are provided in the next section. Section III deals with optimal subcarrier selection and range ambiguity quantification. Experiment and numerical results are provided in section IV, followed by some remarks in section V.

II. Problem Formulation and Analysis

Assume L (>1) subcarriers are reserved for ranging. Practically, the transmitter and receiver introduce an unknown phase $\xi \in [0,2\pi)$ which needs to be estimated via a calibration process in advance. Let r (≥ 0) be the whole path length which is the distance between the transmitter and the target plus the distance between the target and the receiver. Correspondingly, λ_i and $\phi_i(r) \in [-\pi,\pi)$ are wavelength and observed phase at the i-th subcarrier, respectively, $i = 1,2,3,\cdots,L$. Then, the following equation holds, assuming the unknown phase ξ has been compensated:

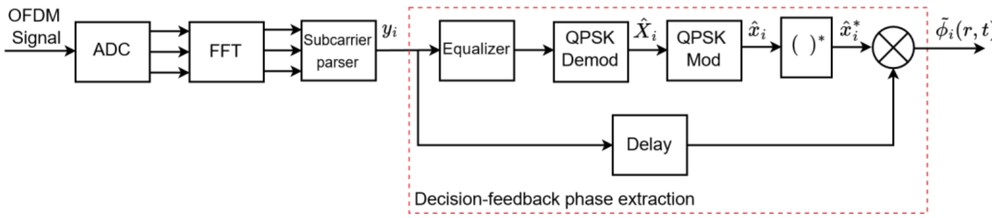

Fig. 2. OFDM receiver with decision-feedback carrier phase extraction (showing only one branch of phase extraction at subcarrier i.).

$$\begin{aligned}\phi_i(r) &= 2\pi\left[\frac{r}{\lambda_i} - round\left(\frac{r}{\lambda_i}\right)\right] \\ &= 2\pi\left[\frac{r}{\lambda_i} - m_i(r)\right],\end{aligned} \tag{1}$$

where $round(\ )$ is the round operation and $m_i(r)$ is the mode number defined as $m_i(r) = round\left(\frac{r}{\lambda_i}\right)$. Note that the mode numbers $m_i(r)$'s are unknown and $\phi_i(r)$ is a periodical function of r with period λ_i, which may cause an ambiguity problem. In practice, the measurement of $\phi_i(r)$ is polluted by phase noise (ignore other possible impairments such as errors caused due to imperfect calibration.)

A. Optimal Ranging

Let $\phi e_i(r,t)$ be the measured phase at time (index) t, and $\nu_i(t)$ the corresponding phase noise value that is sufficiently small such that $\phi e_i(r,t) = \phi_i(r) + \nu_i(t) \in [-\pi,\pi)$. Recalling (1), we can have the following expression

$$\frac{r}{\lambda_i} \approx round\left(\frac{r}{\lambda_i}\right) + \frac{\widetilde{\phi}_i(r,t)}{2\pi}. \tag{2}$$

Define an error metric that is a function of observed phase $\phi e_i(r,t)$ and r', the distance of interest:

$$\begin{aligned}\epsilon_i\left(r', \widetilde{\phi}_i(r,t), \lambda_i\right) &= \phi_i(r') - \widetilde{\phi}_i(r,t) \\ &= 2\pi\left[\frac{r'}{\lambda_i} - round\left(\frac{r'}{\lambda_i}\right) - \frac{\widetilde{\phi}_i(r,t)}{2\pi}\right],\end{aligned} \tag{3}$$

where r is the true range and r' is a variable to be determined. Let $\underset{\sim}{\boldsymbol{\lambda}} = (\lambda_1, \lambda_2, \lambda_3, \cdots, \lambda_L)^T$ be a vector of L wavelengths, and $\boldsymbol{\phi}(r,t) = (\phi_1(r,t), \phi_2(r,t), \phi_3(r,t), \cdots, \phi_L(r,t))^T$ a vector of L phase measurements. Practically, we can define a total error metric $J_\epsilon\left(r', \widetilde{\boldsymbol{\phi}}(r,t), \boldsymbol{\lambda}\right)$ by making use of all L subcarriers and averaging over T observations, if the whole path distance does not change noticeably during the measurement:

$$
\begin{aligned}
&J_{\epsilon}\left(r', \widetilde{\boldsymbol{\phi}}(r,t), \boldsymbol{\lambda}\right) \\
&= \sum_{i=1}^{L} \frac{1}{T} \sum_{t=1}^{T} \epsilon_i^2\left(r', \widetilde{\phi}_i(r,t), \lambda_i\right) \\
&= \sum_{i=1}^{L} \frac{1}{T} \sum_{t=1}^{T} \left[\phi_i(r') - \widetilde{\phi}_i(r,t)\right]^2 \\
&= \sum_{i=1}^{L} \frac{1}{T} \sum_{t=1}^{T} \Big\{ \left[\phi_i(r') - \phi_i(r)\right]^2 \\
&\qquad - \left[\phi_i(r') - \phi_i(r)\right]\nu_i(t) + \nu_i^2(t) \Big\},
\end{aligned} \tag{4}
$$

and then, the range estimate $\hat{r}$ is obtained by

$$
\hat{r} = \underset{r' \in \mathcal{F}}{\operatorname{argmin}}\, J_{\epsilon}\left(r', \widetilde{\boldsymbol{\phi}}(r,t), \boldsymbol{\lambda}\right). \tag{5}
$$

where $\mathcal{F} \in \mathbb{R}$ is a range feasible set.

Considering stationary phase noise and further assuming $\nu_i(t)$ is a zero-mean independent random variable with variance σ_i^2, the range estimation can be asymptotically analyzed. As T goes to infinity, the sample average approaches ensemble average, i.e., $\frac{1}{T}\sum_{t=1}^{T}[\ ]$ in (4) can be replaced by $E[\ ]$ (the statistical expectation):

$$
\begin{aligned}
r^* &= \underset{r' \in \mathcal{F}}{\arg\min} \sum_{i=1}^{L} E\left[\epsilon_i^2\left(r', \widetilde{\phi}_i(r,t), \lambda_i\right)\right] \\
&= \underset{r' \in \mathcal{F}}{\arg\min} \sum_{i=1}^{L} E\left[\left[\phi_i(r') - \phi_i(r)\right]^2 + \sigma_i^2\right] \\
&= \underset{r' \in \mathcal{F}}{\arg\min} \sum_{i=1}^{L} \left[\epsilon_i^2\left(r', \phi_i(r), \lambda_i\right) + \sigma_i^2\right] = r.
\end{aligned} \tag{6}
$$

B. Motion Detection and Estimation

Here motion refers to a micro displacement δ. Consider r and $r+\delta$, and assume δ is sufficiently small such that the two ranges have the same corresponding mode number at each subcarrier (i.e., $round(\frac{r}{\lambda_i}) = round(\frac{r+\delta}{\lambda_i})$). Then, we have the following expressions:

$$
\begin{aligned}
r &= \lambda_i \left[round\left(\frac{r}{\lambda_i}\right) + \frac{\phi_i(r)}{2\pi} \right] \\
&\approx \lambda_i \left[round\left(\frac{r}{\lambda_i}\right) + \frac{\widetilde{\phi}_i(r,t)}{2\pi} \right] \\
&= \lambda_i \left[round\left(\frac{r}{\lambda_i}\right) + \frac{\phi_i(r) + \nu_i(t)}{2\pi} \right],
\end{aligned} \tag{7}
$$

$$
\begin{aligned}
r + \delta &= \lambda_i \left[round\left(\frac{r+\delta}{\lambda_i}\right) + \frac{\phi_i(r+\delta)}{2\pi} \right] \\
&\approx \lambda_i \left[round\left(\frac{r+\delta}{\lambda_i}\right) + \frac{\phi_i(r+\delta) + \nu_i(t+\tau)}{2\pi} \right] \\
&= \lambda_i \left[round\left(\frac{r}{\lambda_i}\right) + \frac{\phi_i(r+\delta) + \nu_i(t+\tau)}{2\pi} \right],
\end{aligned} \tag{8}
$$

where $round(\frac{r}{\lambda_i}) = round(\frac{r+\delta}{\lambda_i})$ has been applied, and τ is a time interval index indicating an observation at a later time. Denote $\phi_i(r+\delta)-\phi_i(r)$ and $\nu_i(t+\tau)-\nu_i(t)$ by $\Delta\phi_i(r)$ and $\Delta\nu_i(t)$, respectively. Accordingly, $\Delta\nu_i(t)$ has a zero-mean and variance $2\sigma_i^2$. The following can be derived from (7) and (8):

$$
\begin{aligned}
\delta &= \frac{\lambda_i}{2\pi} \Delta\phi_i(r) \\
&\approx \frac{\lambda_i}{2\pi} \left[\Delta\phi_i(r) + \Delta\nu_i(t) \right]
\end{aligned} \tag{9}
$$

In practice, δ can be estimated using L subcarriers and T rounds of measurements (if the motion is relatively slow), which leads to an estimate

$$
\begin{aligned}
\widehat{\delta} &= \frac{1}{2\pi LT} \sum_{i=1}^{L} \sum_{t=1}^{T} \lambda_i \left[\Delta\phi_i(r) + \Delta\nu_i(t) \right] \\
&= \delta + \frac{1}{2\pi LT} \sum_{i=1}^{L} \sum_{t=1}^{T} \lambda_i \Delta\nu_i(t).
\end{aligned} \tag{10}
$$

Motion detection for a given threshold θ can be performed straightforward:

$$
\left|\widehat{\delta}\right| \underset{FP}{\overset{TP}{\gtrless}} \theta, \tag{11}
$$

where TP and FP stand for true positive and false positive, respectively.

The quality of this detection can be assessed alternatively using a mechanical signal-to-noise ratio (SNR) defined as

$$
\begin{aligned}
\gamma_{\delta} &= \delta^2 \Big/ E\left[\left\{ \frac{1}{2\pi LT} \sum_{i=1}^{L} \sum_{t=1}^{T} \lambda_i \Delta\nu_i(t) \right\}^2 \right] \\
&= 2T(\pi L\delta)^2 \Big/ \sum_{i=1}^{L} \left(\lambda_i \sigma_i\right)^2.
\end{aligned} \tag{12}
$$

It can be seen that in general the SNR increases as more subcarriers and/or more measurements are used.

For prompt response to fast motion, time-averaging window T has to be sufficiently small, and the extreme case is $T = 1$. Use the WiFi OFDM signal as an example, its OFDM symbol rate is 312.5 kHz, which means the measurement update rate is $312.5/T$ kHz and the maximal rate is 312.5 kHz for $T = 1$. Therefore, according to the Nyquist Theorem, to detect a motion using phase measurement, a rule of thumb is: the motion vibration frequency has to be no more than $0.5 \times 312.5/T = 156.25/T$ kHz.

III. Optimal Selection of Subcarriers and Range Ambiguity Analysis

Let $\boldsymbol{\phi}(r,\boldsymbol{\lambda}) = \big(\phi_1(r,\lambda_i), \phi_2(r,\lambda_i), \cdots, \phi_L(r,\lambda_i)\big)^T$ be a vector of L noiseless phases, Ideally, we want $\phi(r,\lambda)$ be a monotonous function of $r \in \mathrm{F}$ for $\lambda \in \Lambda$, where $\mathrm{F} \in \mathrm{R}$ is a feasible set for range under consideration, and $\Lambda \in \mathrm{R}^{1\times L}$ a pre-defined feasible set for the wavelengths. It can be verified that if r^* is a solution of (1) and a real value u is a least common multiple (LCM) of $\{\lambda_i, i = 1,2,3,\cdots,L\}$, then, unfortunately, $r^* + ku \in \mathrm{F}$, $k = 1,2,3,\cdots$, are solutions of

(1) too, resulting in range ambiguity.

A. Pairwise Error Performance

Recalling (4) and (5), consider a pairwise erroneous event "$J_\epsilon\big(r, \widetilde{\boldsymbol{\phi}}(r,t), \boldsymbol{\lambda}\big) > J_\epsilon\big(r+s, \widetilde{\boldsymbol{\phi}}(r,t), \boldsymbol{\lambda}\big)$" that refers to: given a correct range (r), a wrong range ($r + s$) is chosen based on estimation rule (5). Here a pairwise error corresponds to a pair of ranges r and r+s, and it can be represented by $\{r,s\}$.

Let $Pe(r,s) \triangleq Pr\Big(J_\epsilon\big(r, \boldsymbol{\phi}(r,t), \boldsymbol{\lambda}\big) > J_\epsilon\big(r+s, \boldsymbol{\phi}(r,t), \boldsymbol{\lambda}\big)\Big)$e

e

be the pairwise error probability (chance of making wrong estimation) which can be derived in the following. Define a random variable

$$\begin{aligned}
x(r,s,\boldsymbol{\lambda}) &= J_\epsilon\big(r+s, \widetilde{\boldsymbol{\phi}}(r,t), \boldsymbol{\lambda}\big) - J_\epsilon\big(r, \widetilde{\boldsymbol{\phi}}(r,t), \boldsymbol{\lambda}\big) \\
&= \frac{1}{T}\sum_{i=1}^{L}\sum_{t=1}^{T}\Big[\epsilon_i^2\big(r+s, \widetilde{\phi}_i(r,t), \lambda_i\big) \\
&\qquad -\epsilon_i^2\big(r, \widetilde{\phi}_i(r,t), \lambda_i\big)\Big] \\
&= \frac{1}{T}\sum_{i=1}^{L}\sum_{t=1}^{T}\Big\{\big[\phi_i(r+s) - \phi_i(r)\big]^2 \\
&\qquad -2\big[\phi_i(r+s) - \phi_i(r)\big]\nu_i(t)\Big\} \\
&= \sum_{i=1}^{L}\big[\phi_i(r+s) - \phi_i(r)\big]^2 \\
&\qquad -\frac{2}{T}\sum_{i=1}^{L}\sum_{t=1}^{T}\big[\phi_i(r+s) - \phi_i(r)\big]\nu_i(t) \\
&\triangleq \Gamma_\Phi(r,s,\boldsymbol{\lambda}) + n(r,s,\boldsymbol{\lambda}),
\end{aligned}$$

$$n(r,s,\boldsymbol{\lambda}) = \tfrac{-2}{T}\textstyle\sum_{i=1}^{L}\sum_{t=1}^{T}\big[\phi_i(r+s) - \phi_i(r)\big]\nu_i(t) \tag{13}$$

whereis the noise part of $x(r,s)$, and the constant part is given by

$$\begin{aligned}
\Gamma_\Phi(r,s,\boldsymbol{\lambda}) &= \sum_{i=1}^{L}\big[\phi_i(r+s) - \phi_i(r)\big]^2 \\
&= \Big\|\boldsymbol{\phi}(r+s,\boldsymbol{\lambda}) - \boldsymbol{\phi}(r,\boldsymbol{\lambda})\Big\|_2^2
\end{aligned} \tag{14}$$

It can be found that $n(r,s,\lambda)$ is a zero-mean random variable

$$\begin{aligned}
\sigma_x(r,s,\boldsymbol{\lambda}) &= \overline{T} \quad {}_{i=1} \\
&= \frac{16\pi^2}{T}\sum_{i=1}^{L}\sigma_i^2\Big\{\Big[\frac{s}{\lambda_i} + round\Big(\frac{r}{\lambda_i}\Big) \\
&\qquad -round\Big(\frac{r+s}{\lambda_i}\Big)\Big]^2\Big\}
\end{aligned} \tag{15}$$

with variance:^{2} $\quad 4\sum^{L}\sigma_i^2[\phi_i(r+s) - \phi_i(r)]^2$

Therefore, the pairwise error probability conditioned on λ can be calculated by

$$\begin{aligned}
Pe(r,s|\boldsymbol{\lambda}) &= Pr\big(x(r,s,\boldsymbol{\lambda}) < 0\big) \\
&= Pr\big(\Gamma_\Phi(r,s,\boldsymbol{\lambda}) + n(r,s,\boldsymbol{\lambda}) < 0\big) \\
&= Q\Big(\frac{\Gamma_\Phi(r,s,\boldsymbol{\lambda})}{\sigma_x(r,s,\boldsymbol{\lambda})}\Big), \\
Q(z) &= \int_z^\infty \frac{1}{\sqrt{2\pi}}e^{-\frac{y^2}{2}}dy.
\end{aligned} \tag{16}$$

B. Optimal Set of Wavelengths

Note that $\Gamma_\Phi(r,s,\lambda)$ defined in (14) reflects phase change corresponding to a distance change from r to $r + s$, thus it can be used as a metric in searching for the best combination of wavelengths. Practically, to minimize range ambiguity, the search strategy can be formulated as a max-min optimization problem by selecting the best combination of wavelengths for the worst case:

$$\lambda^* = \operatorname*{argmax}_{\lambda\in\Lambda}\ \min_{r,r+s\in\mathrm{F}}\ \Gamma_\Phi(r,s,\lambda) \tag{17}$$

$$s.t.\ |s| > s_0$$

where $s_0 > 0$ is a maximally tolerable range error to reflect some error tolerance in range estimation. It is practically acceptable if the difference between two range estimates is within s_0. A rule of thumb for selecting s_0 is that it should no less than the order of measurement resolution. We will not pursue a closed-form solution to (17), rather use (17) to search the best wavelengths for relatively small sets of F and Λ.

C. Ambiguity Quantification

The ambiguity can be quantitatively measured using $\Gamma_\Phi(r,s,\lambda)$. Given F, Λ, s_0, and the best wavelengths λ^*, there is the worst case which deserves more concern. Let (r',s') represent the worst case, i.e.,

$$(r',s') = \operatorname*{argmin}_{r,r+s\in\mathrm{F}}\Gamma_\Phi(r,s,\lambda^*) \tag{18}$$

$$s.t.\ |s| > s_0$$

The worst-case ambiguity level for any $\boldsymbol{\lambda}$ is $\Gamma_\Phi(r', s', \boldsymbol{\lambda})$.

An even better ambiguity measure is the pairwise error probability. Recalling (9), the pairwise error probability for the worst case can be expressed as $Pe(r',s'|\lambda^*) = Q\left(\frac{\Gamma_\phi(r',s',\boldsymbol{\lambda}^*)}{\sigma_x(r',s',\boldsymbol{\lambda}^*)}\right)$. Furthermore, it can be proved (see Appendix) that the following inequalities hold if phase noise has the same strength over different subcarriers:

$$Pe(r,s|\lambda^*) \leq Pe(r,s|\lambda), \tag{19}$$

$$Pe(r,s|\lambda^*) \leq Pe(r',s'|\lambda^*), \tag{20}$$

which basically says, (1) for any given estimation error, employing the best set of wavelengths minimizes the chance of that error; and (2) when the best set of wavelengths are chosen, any pairwise error probability is no greater than the worst-case pairwise error probability.

IV. Experimental and Analytical Results

A. Precise Ranging Using Decision Feedback on Multiple Data Subcarriers

A standard OFDM based communication system reserves pilot subcarriers for channel state information (CSI) estimation, and they can be used for sensing as well. However, there are reasons that we may need to use the data (non-pilot) subcarriers as well for sensing purpose: 1) more subcarriers are employed to combat phase noise and improve detection sensitivity and estimation accuracy; and 2) the reserved pilot subcarriers are usually not optimal in terms of range ambiguity. In this paper we consider measuring range-related phases over multiple subcarriers including data subcarriers, and combining the phases for distance estimation.

We propose and implement a decision-feedback based phase extraction technique to estimate the range-related phases as shown in Fig. 2, where the regular communication part is not omitted and only one branch of phase estimation is shown. The subcarrier parser selects the data subcarriers from the FFT of the baseband OFDM signal. Then, for each subcarrier, the decision feedback technique is used to remove the unknown transmitted data symbols from the subcarrier, leaving a residual phase $\tilde{\phi}_i(r,t)$ that reflects the length of the whole propagation path.

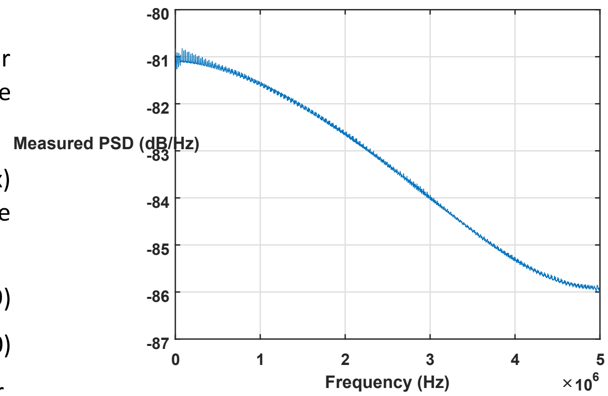

Fig. 3. Phase noise PSD of a randomly selected data subcarrier.

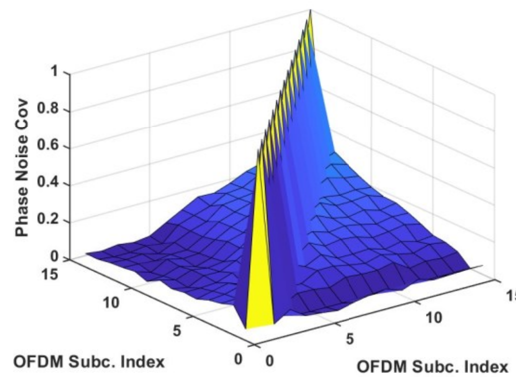

Fig. 4. Normalized phase noise covariance of selected subcarriers.

B. Phase Noise Measurement and Analysis

Assumption of independent and stationary phase noise has been used in Section III. As mentioned earlier, phases extracted from multiple subcarriers are combined (e.g., by averaging) to improve estimation quality. However, this argument is based on the fact that the phase noise over different subcarriers are independent or weakly dependent on each other. The orthogonality of OFDM subcarriers is in favor of this prerequisite condition, but experimentally verifying it is still desired. 802.11a standard for the OFDM transmission and reception is followed in conducting our experiment, and a small test setup is implemented using USRP software defined radios (SDRs).

We measure the power spectrum density (PSD) of the phase noise at different data subcarriers and test the characteristics of the noise random process. Fig. 3 shows the PSD of a randomly selected data subcarrier. By processing the measured data, it is found that both the mean and variance of the phase noise do not change much over time, suggesting that the phase noise can be viewed as a wide-sense stationary (WSS) random process. Also, we apply cross-covariance to the phase noise over different subcarriers to check its correlations. As shown in Fig. 4, the phase noise covariance matrix (normalized) is nearly an identity matrix, which means that the phase noise at a subcarrier is indeed quite independent of that at any other subcarrier.

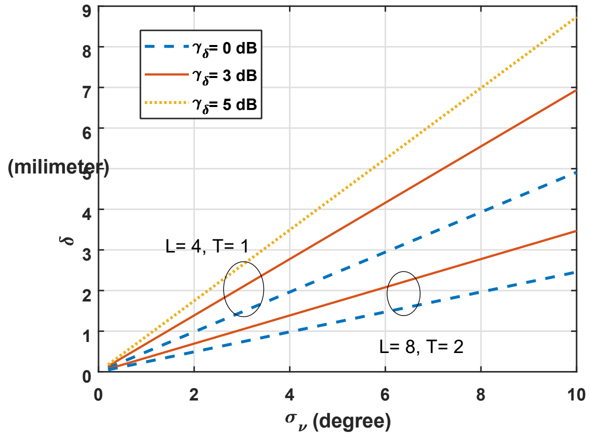

Fig. 5. Sensitivity of motion detection and estimation.

Furthermore, the Gaussianity of the phase noise in terms of Skewness and Kurtosis is shown below:

1) Skewness = 0.641 (zero if ideal Gaussian process); 2) Kurtosis = 2.646 (3 if ideal Gaussian process).

In conclusion, the phase noise of the SDR version of OFDM system can be roughly viewed as an independent and identically distributed (iid) WSS Gaussian random process.

C. Motion Detection and Range Ambiguity Assessment

Fig. 5 is generated based on (12), showing the sensitivity level of motion detection for a desired estimation quality represented by γ_δ. For instance, if we want γ_δ = 3 dB or above, then at phase noise standard deviation σ_ν = 3.5 degree, the minimum displacement is δ = 2.5 mm. Of course, smaller displacement can be estimated as (L,T) increase.

Four test cases are considered for simulation and defined as follows. WiFi pilots: use of four WiFi pilot subcarriers for ranging; WiFi pilots + one: in addition to the four WiFi pilot subcarriers, optimally use one data subcarrier for ranging; Optimal: the proposed max-min based method; and Worst: the worst combination of four subcarriers.

TABLE I

RESULTSOFFOURTESTCASES

L = 4 or 5, T = 1, s_0 = 1.25 cm, F = [5,20] m, Λ = {52 wavelengths according to the WiFi (IEEE 802.11a) standard}.

Test cases	Subcarrier indexes	r',s'	p ′,s′,λ) Γ_Φ(r
WiFi pilots	-21, -7, 7, 21	16.0094, 0.1250	1.4674
WiFi pilots+one	-26 -21, -7, 7, 21	16.0094, 0.1250	1.9075
Optimal, L = 4	-19, 19, 23, 26	15.8844, 0.1250	2.0577
Optimal, L = 5	-23, -15, 10, 25, 26	15.8844, 0.1250	2.1760
Worst, L = 4	-3, 3, 9, 15	15.9156, 0.1250	0.8437

Table I shows ambiguity related results generated based on (17) and (18) for the condition specified by L,T,s_0,F and Λ. One can see that selection of subcarriers does matter: use of WiFi pilot subcarriers for phase-based ranging is not optimal, but the norm of phase difference ($^{\mathrm{p}}\Gamma_\Phi(r',s',\lambda)$) can be improved by adding one data subcarrier; increasing the number of subcarriers improves performance in general; and a bad selection of subcarriers degrades performance. Range ambiguity assessed in pairwise error probability for the four test cases is shown in Fig. 6. Under this particular test condition and at pairwise error probability 10^{-2} , the gap between the worst and the optimal corresponds to a change of the phase noise standard deviation from 1.5 degrees 2.3 degrees. Of course, the gap depends on the test condition, and what we really care about is the ambiguity level corresponding to the actual measured phase noise strength.

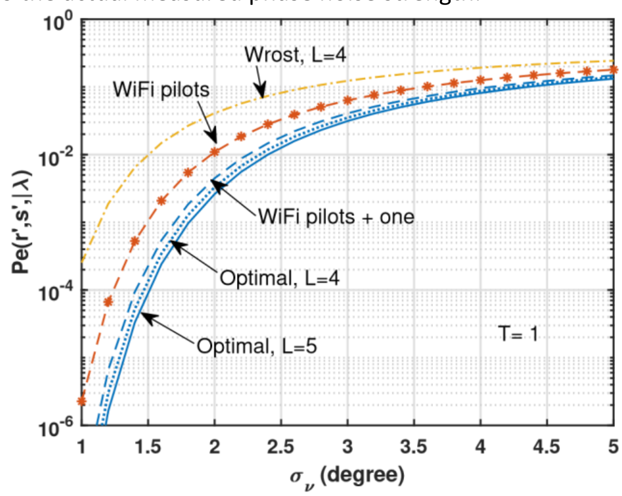

Fig. 6. Range ambiguity assessment in pairwise error probability.

V. Remarks

There is no doubt that sensing information as an addon with nearly no cost to an IoT system can benefit all engaged parties. This paper lays out an analytical framework for phase-based ranging along with assessment using both analysis and experiment. To the best of our knowledge, it is the first time that optimal selection of subcarrier frequencies is formulated as a max-min optimization problem, and range ambiguity measured in pairwise error probability is assessed quantitatively against phase noise. The phase noise becomes a performance-limiting factor as we attempt to achieve an ultra-fine ranging resolution. To overcome that a decisionfeedback phase extraction technique is proposed so that an excessive number of subcarriers including data subcarriers can be employed constructively. Although we follow the WiFi standard in performance evaluation and experiment, the proposed analytical framework can be applied to other wireless communication standards, such 5G NR-Sub 6GHz that can accommodate 240 subcarriers. Due to page limitation, this paper mainly focuses on a few theoretical and experimental issues. We will continue working to solve the max-min problem (17) efficiently. Many related and interesting topics, such as comparison with some existing approaches, calibration, beamforming and beam sweeping, robust localization, target tracking, motion-directed resource allocation, and impact of multipath, need to be further investigated. We will discuss some of these and report experiment work in detail in a separate paper.

APPENDIX–PROOF OF (19) AND (20)

Recalling (16), $Pe(r,s|\lambda)$ monotonically decreases as $\frac{\Gamma_\Phi(r,s,\boldsymbol{\lambda})}{\sigma_x(r,s,\boldsymbol{\lambda})}$ increases. Assume $\sigma_i^2 = \sigma_\nu^2,\ i = 1,2,3,\cdots,L$, then, according to (14) and (15), we have

$$\begin{aligned}\sigma_x^2(r,s,\boldsymbol{\lambda}) &= \frac{4}{T}\sum_{i=1}^{L}\sigma_\nu^2\big[\phi_i(r+s)-\phi_i(r)\big]^2\\ &= \frac{4\sigma_\nu^2}{T}\sum_{i=1}^{L}\big[\phi_i(r+s)-\phi_i(r)\big]^2\\ &= \frac{4\sigma_\nu^2}{T}\Big\|\boldsymbol{\phi}(r+s,\boldsymbol{\lambda})-\boldsymbol{\phi}(r,\boldsymbol{\lambda})\Big\|_2^2\\ &= \frac{4\sigma_\nu^2}{T}\Gamma_\Phi(r,s,\boldsymbol{\lambda}).\end{aligned} \tag{21}$$

$$\frac{\Gamma_\Phi(r,s,\boldsymbol{\lambda})}{\sigma_x(r,s,\boldsymbol{\lambda})} = \frac{\sqrt{T\cdot\Gamma_\Phi(r,s,\boldsymbol{\lambda})}}{2\sigma_\nu}. \tag{22}$$

According to (16) and (22), $\frac{\Gamma_\Phi(r,s,\boldsymbol{\lambda}^*)}{\sigma_x(r,s,\boldsymbol{\lambda}^*)} \geq \frac{\Gamma_\Phi(r,s,\boldsymbol{\lambda})}{\sigma_x(r,s,\boldsymbol{\lambda})}$ holds and it is a sufficient and necessary condition for (18); similarly, according to (17) and (22), we have $\frac{\Gamma_\Phi(r,s,\boldsymbol{\lambda}^*)}{\sigma_x(r,s,\boldsymbol{\lambda}^*)} \geq \frac{\Gamma_\Phi(r',s',\boldsymbol{\lambda}^*)}{\sigma_x(r',s',\boldsymbol{\lambda}^*)}$, which implies (19) holds.

REFERENCES

[1] F. Liu, Y. Cui, C. Masouros, J. Xu, T. X. Han, Y. C. Eldar, and S. Buzzi, "Integrated sensing and communications: Towards dual-functional wireless networks for 6g and beyond," *IEEE Journal on Selected Areas in Communications*, 2022.

[2] N. Patwari, J. N. Ash, S. Kyperountas, A. O. Hero III, R. L. Moses, and N. S. Correal, "Locating the nodes: cooperative localization in wireless sensor networks," *Signal Processing Magazine, IEEE*, vol. 22, no. 4, pp. 54–69, 2005.

[3] A.-M. Roxin, J. Gaber, M. Wack, and A. N. S. Moh, "Survey of wireless geolocation techniques," in *IEEE Globecom Workshops*, 2007, pp. 9–Pages.

[4] K. W. Cheung, H.-C. So, W.-K. Ma, and Y.-T. Chan, "Least squares algorithms for time-of-arrival-based mobile location," *Signal Processing, IEEE Transactions on*, vol. 52, no. 4, pp. 1121–1130, 2004.

[5] S. Gezici, Z. Tian, G. B. Giannakis, H. Kobayashi, A. F. Molisch, H. V. Poor, and Z. Sahinoglu, "Localization via ultra-wideband radios: a look at positioning aspects for future sensor networks," *Signal Processing Magazine, IEEE*, vol. 22, no. 4, pp. 70–84, 2005.

[6] ˙I. Güvenç and C.-C. Chong, "A survey on TOA based wireless localization and NLOS mitigation techniques," *Communications Surveys & Tutorials, IEEE*, vol. 11, no. 3, pp. 107–124, 2009.

[7] G. Mao, B. Fidan, and B. D. Anderson, "Wireless sensor network localization techniques," *Computer networks*, vol. 51, no. 10, pp. 2529–2553, 2007.

[8] A. Coluccia and F. Ricciato, "RSS-based localization via Bayesian ranging and iterative least squares positioning," *Communications Letters, IEEE*, vol. 18, no. 5, pp. 873–876, 2014.

[9] L. Chen, X. Zhou, F. Chen, L.-L. Yang, and R. Chen, "Carrier phase ranging for indoor positioning with 5G NR signals," *IEEE Internet of Things Journal*, vol. 9, no. 13, pp. 10908–10919, 2021.

[10] J. Li, M. Liu, S. Shang, X. Gao, and J. Liu, "Carrier phase positioning using 5G NR signals based on OFDM system," in *2022 IEEE 96th Vehicular Technology Conference (VTC2022-Fall)*. IEEE, 2022, pp. 1–5.

[11] S. Fan, W. Ni, H. Tian, Z. Huang, and R. Zeng, "Carrier phase-based synchronization and high-accuracy positioning in 5G new radio cellular networks," *IEEE Transactions on Communications*, vol. 70, no. 1, pp. 564–577, 2021.

[12] W. Kim, J. Park, and J. Cho, "Implementation of carrier phase positioning for 5G OFDM system," in *2022 13th International Conference on Information and Communication Technology Convergence (ICTC)*.
IEEE, 2022, pp. 2058–2061.